Bull. Mater. Sci., Vol. 32, No. 5, October 2009, pp. 531–536. © Indian Academy of Sciences.

Effect of cerium and thermomechanical processing on microstructure and mechanical properties of Fe–10·5Al–0·8C alloy

R G BALIGIDAD and SHIVKUMAR KHAPLE*
Defence Metallurgical Research Laboratory, Hyderabad 500 058, India

MS received 1 September 2008; revised 30 October 2008

Abstract. **The effect of cerium content and thermomechanical processing on structure and properties of Fe–10·5 wt.%Al–0·8 wt%C alloy has been investigated. Alloys were prepared by a combination of air induction melting with flux cover (AIMFC) and electroslag remelting (ESR). The ESR ingots were hot-forged and hot-rolled at 1373 K as well as warm-rolled at 923 K and heat-treated. Hot-rolled, warm-rolled and heat treated alloys were examined using optical microscopy, scanning electron microscopy (SEM) and X-ray diffraction to understand the microstructure of these alloys. The ternary, Fe–10·5 wt.%Al–0·8 wt.%C alloy showed the presence of two phases; Fe–Al with *bcc* structure, and large volume fraction of $Fe_3AlC_{0.5}$ precipitates. Addition of cerium to Fe–10·5 wt.%Al–0·8 wt.%C alloy resulted in three phases, the additional phase being small volume fraction of fine cerium oxy-carbide precipitates. Improvement in tensile elongation from 3–6·4% was achieved by increasing the cerium content from 0·01–0·2 wt.% and further improvement in tensile elongation from 6·4–10% was achieved by warm-rolling and heat treatment.**

Keywords. **Iron aluminides; cerium addition; air induction melting; electroslag remelting; EPMA.**

1. Introduction

Iron aluminides are being developed for elevated temperature structural applications for temperatures up to 873 K (Mendiratta *et al* 1987; Stoloff 1998; Schwaiger *et al* 2003). They also provide potential replacement for the more expensive heat-resistant alloys such as austenitic and ferritic steels containing strategic elements like nickel and chromium. However, poor ambient temperature ductility, poor toughness and poor creep properties have limited their acceptance for many structural applications. Recent developments have indicated that the room temperature ductility of Fe–16 wt.%Al alloy can be improved by the addition of chromium (McKamey and Liu 1990). The micro-alloying of cerium to Fe–16 wt.%Al alloy has resulted in significant improvement in both strength and ductility (Yangshan *et al* 1995, 1996; Kratochvil *et al* 1999). It has been shown that the addition of carbon to Fe–(8·5–16 wt.%) Al alloys leads to an improved strength, creep resistance, machinability and resistance to environmental embrittlement (Baligidad *et al* 1997, 1998a, b; Schneider *et al* 2005). Recently a process route has been established to produce Fe–Al–C alloys containing reactive elements like Ce and also shown that addition of 0·2 wt%Ce (to Fe–Al–C alloys) leads to significant improvement in ductility (Baligidad and Radhakrishna 2002a, b). The purpose of the present paper is to report the effect of cerium concentration and thermomechanical processing on microstructure and mechanical properties of Fe–10·5 wt.%Al–0·8 wt.%C alloy at ambient temperature and at 873 K as well as creep and stress rupture properties at 873 K and 140 MPa.

2. Experimental

Four alloys with nominal compositions listed in table 1 were prepared by a combination of air induction melting with flux cover (AIMFC) and electroslag remelting (ESR) as described elsewhere (Baligidad *et al* 1998a; Baligidad and Radhakrishna 2002a, b) (all the compositions are in wt.% unless otherwise specified). The 80 mm diameter ESR ingots were held in a furnace at 1373 K for 1 h and hot-forged to a thickness of 25 mm and subsequently hot-rolled at 1373 K to 12 mm thick plate. The ESR hot-rolled thick sections of Fe–10·5Al–0·8C–0·2Ce alloy was further hot-rolled at 1373 K to a thickness of 4 mm and warm-rolled at 923 K to a thickness of 2 mm. The 2 mm thick warm-rolled section was annealed at 973 K and 1273 K for 1 h and furnace cooled to room temperature. The details of hot-working are given elsewhere (Baligidad *et al* 1994).

Longitudinal section of hot-rolled 12 mm thick sheets of ESR Fe–10·5Al–0·8C–0·01Ce (alloy 2) and Fe–10·5Al–0·8C–0·04Ce (alloy 3) alloys as well as hot and

*Author for correspondence (sikaple@yahoo.com)

warm-rolled 2 mm thick sheets of ESR Fe–10·5 Al–0·8C–0·2Ce alloy were cut using bi-metallic band-saw blade. The cut-off sections were mechanically polished to 0·5 μm grade diamond powder finish and etched with an etchant composed of 33% HNO_3 + 33% CH_3COOH + 33% H_2O + 1% HF by volume for microstructural examination by optical microscopy and scanning electron microscopy (SEM). For X-ray diffraction (XRD) studies in a Philips 3710 Diffractometer, the hot-rolled ESR ingots were machined and powder samples were prepared from the turnings ground and sieved to –220 mesh (75 μm) size. The bulk hardness measurements were made on the hot-rolled, and warm-rolled and heat-treated microscopy samples using a Vickers hardness machine with 30 kg load. Longitudinal ASTM-E 8M round tensile specimens of 4·0 mm gauge diameter and 20 mm gauge length and flat tensile specimens of 10 mm gauge length were prepared from hot-rolled ESR ingots of alloys 2–4 as well as from warm-rolled and heat-treated ESR ingot of alloy 4. Tensile tests were carried out at room temperature and at 873 K in an Instron Universal testing machine at a strain rate of $0{\cdot}8 \times 10^{-4}$ s^{-1}. The details of sample preparation and testing procedure are given elsewhere (Khaple *et al* 2007). Constant load creep and stress rupture tests were carried out on hot-rolled ESR ingots of alloys 2, 3 and 4. For these tests specimens of 5 mm gauge diameter and 25 mm gauge length were machined and polished. The details of sample preparation and creep testing procedures are given elsewhere (Khaple *et al* 2006). The tensile fracture surfaces were examined in SEM.

3. Results and discussion

Scanning electron micrographs of hot-rolled ESR ingots of alloys 2 and 3 are shown in figures 1 and 2. For the purpose of comparison, micrographs of alloys 1 and 4 of hot-rolled ESR ingots are included from our previous work (Baligidad and Radhakrishna 2002b). Scanning electron micrographs showed the presence of significant amounts of precipitates in the hot-rolled ESR ingots of alloys 1–4 (figure 1). The back scattered electron micrographs of SEM revealed the presence of two types of precipitates in alloys 2–4 (figure 2) whereas alloy 1 exhibited only one type of precipitates. The matrix and large volume fraction of precipitates, which appear relatively dark in BSE images of SEM in alloys 1–4, are confirmed to be Fe–Al(α) and $Fe_3AlC_{0·5}$ phases, respectively by X-ray diffraction (figure 3). The fine, very small volume fraction of bright precipitates observed in BSE images of SEM in alloys 2–4, were identified previously, by one of the authors, as cerium-oxycarbide precipitates by EPMA (Baligidad *et al* 1998b). The precipitates were distributed uniformly throughout the matrix in the hot-rolled ingots of alloys 1–4. In case of cerium addition to the hot-rolled Fe–10·5Al–0·8C alloy, the carbide particles were much finer and more globular. It indicates that addition of

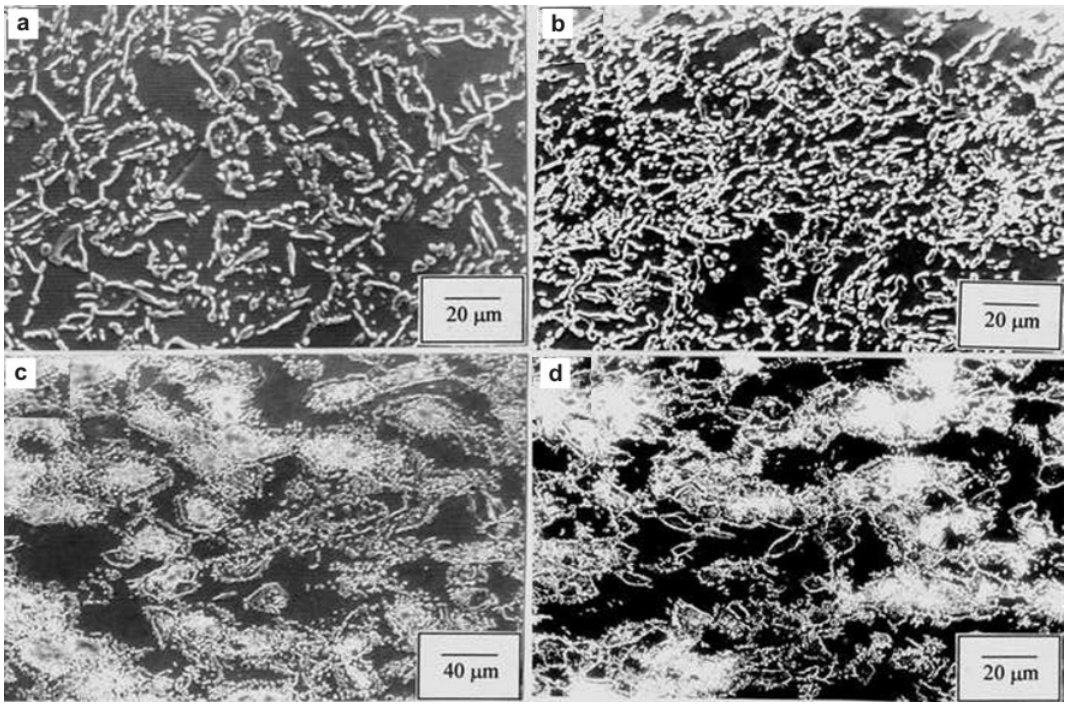

Figure 1. SEM secondary electron micrographs showing large volume fraction of precipitates in hot-rolled ESR ingots of (**a**) Fe–10·5Al–0·8C, (**b**) Fe–10·5Al–0·8C–0·01Ce, (**c**) Fe–10·5Al–0·8C–0·04Ce and (**d**) Fe–10·5Al–0·8C–0·2Ce alloys.

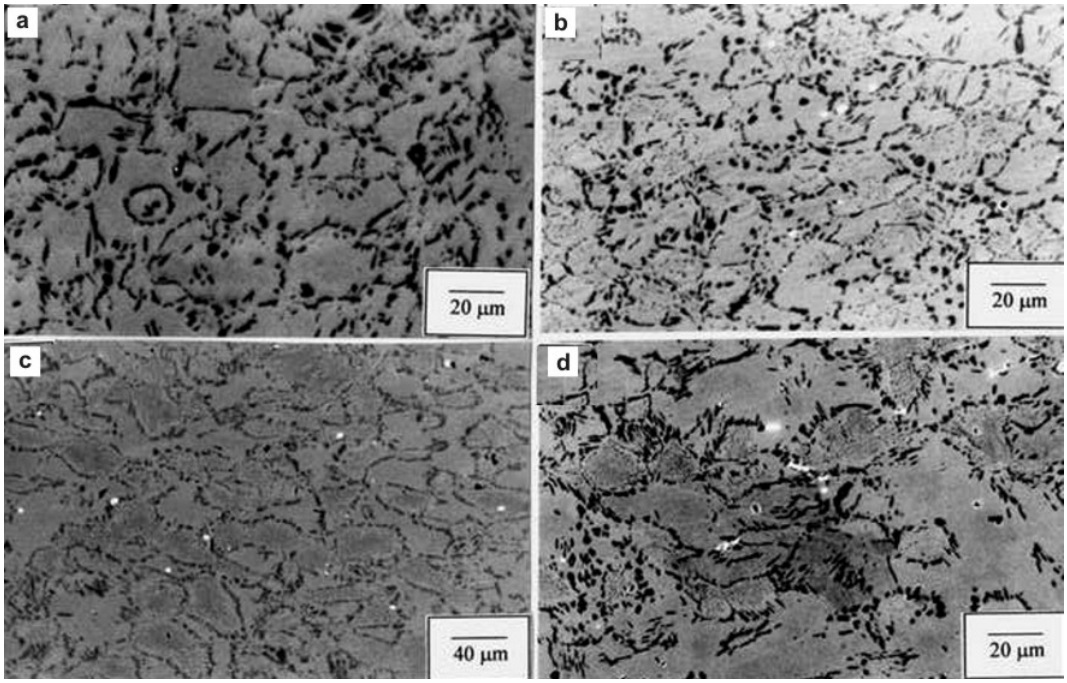

Figure 2. SEM back-scattered electron micrographs showing large volume fraction of dark precipitates in hot-rolled ESR ingots of (**a**) Fe–10·5Al–0·8C alloy and large volume fraction of dark precipitates and small volume fraction of bright precipitates in hot-rolled ingots of (**b**) Fe–10·5Al–0·8C–0·01Ce, (**c**) Fe–10·5Al–0·8C–0·04Ce and (**d**) Fe–10·5Al–0·8C–0·2Ce alloys.

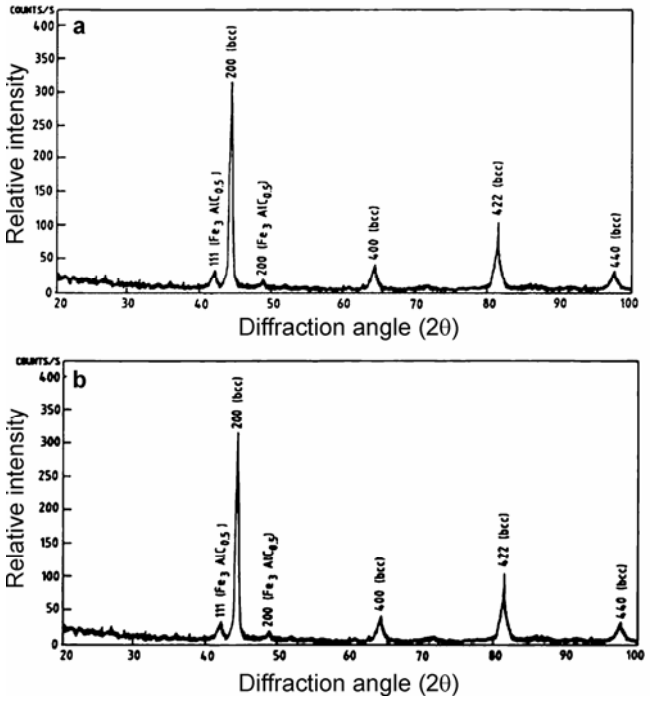

Figure 3. XRD traces using Cu-Kα radiation showing *bcc* and $Fe_3AlC_{0.5}$ peaks in **a**. Fe–10·5Al–0·8C and **b**. Fe–10·5Al–0·8C–0·2Ce alloys. Similar peaks were observed in Fe–10·5Al–0·8C–0·01Ce and Fe–10·5Al–0·8C–0·04Ce alloys.

cerium has influenced the size and morphology of the carbides. This can be explained based on the well-known effect of Ce addition in modifying the carbide/graphite morphology in cast iron. All the hot-rolled (alloys 1–4) alloys possess recrystallized grains. This was expected because the hot-rolling of the alloys was preformed at high temperatures (1373 K), where dynamic recrystallization has taken place. The microstructure of warm-rolled and heat-treated ESR ingot of alloy 4 (Fe–10·5Al–0·8C–0·02Ce) showed very fine and more uniformly distributed $Fe_3AlC_{0.5}$ precipitates as compared to hot-rolled ESR ingots of alloy 4 (figure 4).

The hardness values, room temperature and 873 K tensile test results of hot-rolled ESR ingots of alloys 2 and 3 as well as hardness and room temperature tensile properties of warm-rolled and heat treated ESR ingots of alloy 4 are listed in table 1. The creep and stress rupture results of alloys 2, 3 and 4 are presented in table 2. Each hardness data point reported here represents an average of 5 measurements, each tensile and creep rupture data point reported here represents an average of two tests. For the purpose of comparison, hardness and room temperature and 873 K tensile data of hot-rolled ESR ingots of alloys 1 and 4 tested under similar condition are included in table 1 from the literature (Baligidad and Radhakrishna 2002a, b). It can be seen from tables 1 and 2 that the base alloy Fe–10·5Al–0·8C (alloy 1) exhibits poor room temperature ductility and creep properties. Cerium addition to the base alloy has resulted in significant improvement in room temperature ductility. The tensile elongation of the base alloy increased significantly (1·8–3·0%) by the

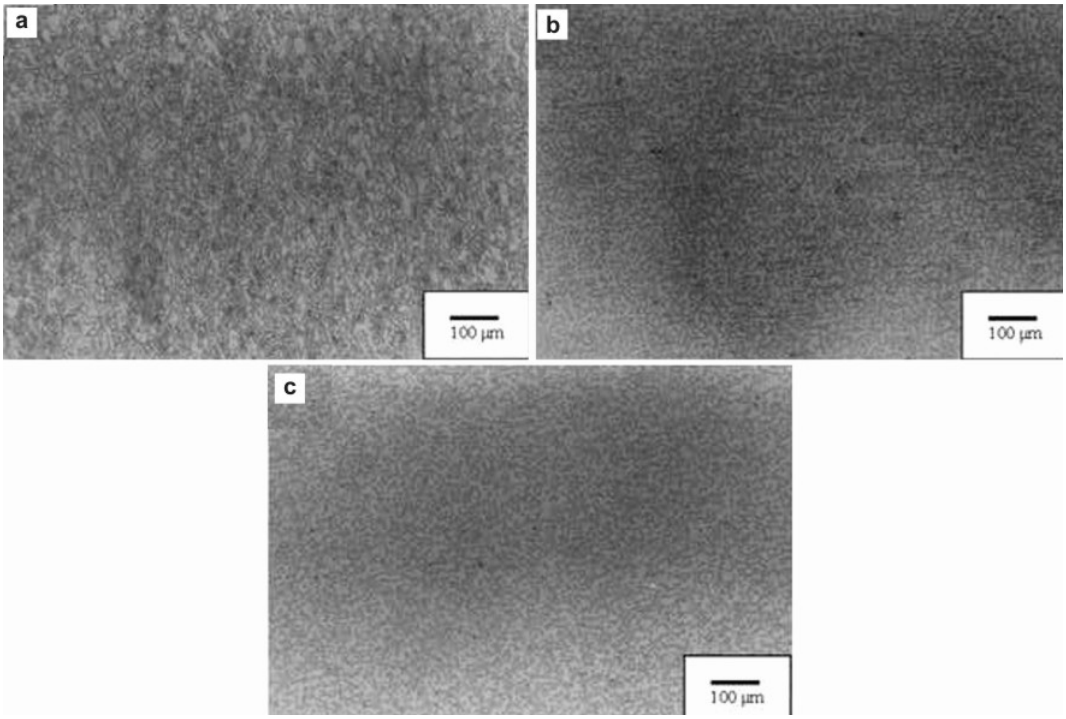

Figure 4. Optical micrographs of **a**. hot-rolled 12 mm thick, **b**. hot and warm-rolled and heat treated (973 K/1h/FC) 2 mm thick and **c**. hot and warm-rolled and heat treated (1273 K/1h/FC) 2 mm thick ESR Fe–10·5Al–0·8C–0·2Ce alloy showing $Fe_3AlC_{0.05}$ precipitates.

Table 1. Effect of cerium as well as warm-rolling and heat treatment on tensile properties of Fe–10·5Al–0·8 C alloy.

Alloy	Composition (wt.%)	Processing condition	Hardness (HV)	Tensile properties (RT)			Tensile properties (873 K)		
				UTS (MPa)	YS (MPa)	El (%)	UTS (MPa)	YS (MPa)	El (%)
1	Fe–10·5Al–0·8C	Hot-rolled*	315	833	720	1·8	318	300	60
2	Fe–10·5Al–0·8C–0·01Ce	Hot-rolled*	299	897	732	3·0	349	323	70
3	Fe–10·5Al–0·8C–0·04Ce	Hot-rolled*	310	914	738	4·1	300	294	82
4a	Fe–10·5Al–0·8C–0·2Ce	Hot-rolled*	290	844	660	6·4	292	275	90
4b	Fe–10·5Al–0·8C–0·2Ce	Hot + warm-rolled** + Heat-treated***	302	789	594	10	–	–	–
4c	Fe–10·5Al–0·8C–0·2Ce	Hot + warm-rolled** + Heat-treated****	288	765	584	9	–	–	–

*80 mm dia ESR ingot hot-forged at 1373 K to 25 mm thick and hot-rolled at 1373 to 12 mm thick plate; **80 mm dia ESR ingot hot-forged at 1373 K to 25 mm thick, and hot-rolled at 1373 to 4 mm thick, warm-rolled at 923 K to 2 mm; ***heat treated at 973 K for 1 h and furnace cooled to room temperature; ****heat treated at 1273 K for 1 h and furnace cooled to room temperature

addition of 0·01 wt.% cerium. By comparing alloys 2, 3 and 4 (table 1), it can be seen that the room temperature tensile elongation increased with increasing cerium content (table 1 and figure 5). The highest tensile elongation of 6·4% was obtained from alloy 4 which contained 0·2 wt.%Ce. Warm-rolling and heat treatment of alloy 4 resulted in further increase in tensile elongation from 6·4–10% without significant loss in strength. The increase in tensile elongation was also observed in high temperature tensile tested hot-rolled ESR (alloys 1–4) alloys (table 1). The tensile elongation of all the four hot-rolled alloys at 873 K is significantly higher (60–90%) as compared to room temperature (1·8–6·4%). The transgranular cleavage failure was observed in the tensile samples of all the four alloys tested at room temperature. At 873 K the failure mode changed to ductile dimple (figure 6).

Table 2. Effect of cerium on creep properties of hot-rolled Fe–10·5Al–0·8C alloy.

Alloy	Composition (wt.%)	Creep properties (873 K, 140 MPa)		
		Life (h)	MCR (%/h)	El (%)
Alloy 1	Fe–10·5Al–0·8C	2·4	11	58
Alloy 2	Fe–10·5Al–0·8C–0·01Ce	2·5	8·0	94
Alloy 3	Fe–10·5Al–0·8C–0·04Ce	2·6	9·2	88
Alloy 4	Fe–10·5Al–0·8C–0·2Ce	2·9	8·6	110

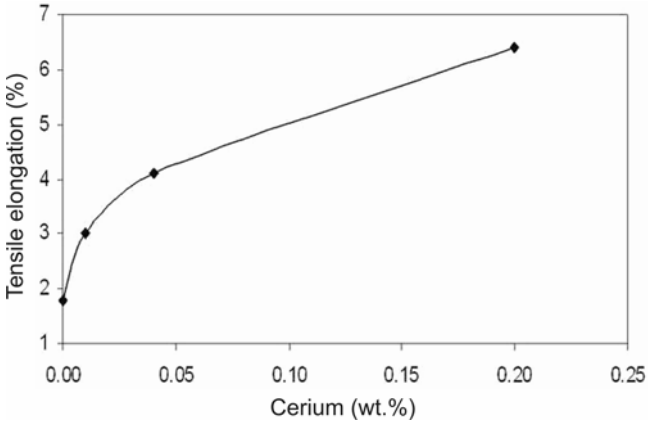

Figure 5. Effect of cerium on tensile elongation of hot-rolled 12 mm thick sheet of ESR Fe–10·5Al–0·8C alloy.

It can be seen from table 1 that alloys 1, 2 and 3 exhibit 299–315 Hv hardness, 720–738 MPa yield strength at room temperature and 294–323 MPa yield strength at 873 K, whereas alloy 4, containing 0·2 wt.%Ce, exhibits slightly lower (290 Hv) hardness and poor yield strength at room temperature (660 MPa) and 873 K (275 MPa). This study indicates that addition of cerium up to 0·04 wt.% did not improve the strength, whereas addition of 0·2 wt.%Ce has resulted in reduction of yield strength both at room temperature and 873 K. It has been reported (Yangshan *et al* 1996) earlier that the addition of small (0·15%) amount of cerium to carbon free Fe–16Al alloy resulted in significant improvement (8·5–14·3%) in tensile elongation, and marginal improvement in yield strength (470–505 MPa). The reasons for poor yield strength observed in the Fe–10·5Al–0·8C–0·2Ce alloy in the present work have not been understood yet. It can be seen from table 2 that addition of 0·04–0·2 wt%Ce to the base alloy (Fe–10·5Al–0·8C) did not exhibit any significant improvement in either creep life or minimum creep rate. However, alloys containing cerium exhibited significant reduction in area accompanied by necking and elongation of 94–110% as compared to the base alloy (58%).

In the present work the mechanisms by which cerium ductilizes the high carbon Fe–10·5Al alloy has also not been understood. However, it is felt that the ductilization by Ce may be due to the formation of fine and globular carbide ($Fe_3AlC_{0·5}$) grains or due to the improved resistance to environmental embrittlement offered by the modification of surface oxide by cerium (Yangshan *et al* 1996). Fe–Al alloys containing more than 8 wt.%Al are known to be susceptible to environmental embrittlement in the presence of atmospheric moisture (Baligidad *et al* 1996; Chiu *et al* 2000). This embrittlement has been proposed to be due to diffusion of nascent hydrogen liberated by the chemical reaction between aluminum present in the alloy and the atmospheric moisture. Cerium addition may accelerate the formation of Al oxide which passivates the specimen surface, thus preventing hydrogen diffusion into the specimen. This may also be attributed to the grain refinement during solidification by precipitation of high melting cerium-rich particles. In the present study, further improvement in the room temperature ductility (6·4–10%) achieved in alloy 4 (Fe–10·5Al–0·8C–0·2Ce) by hot rolling to 4 mm thickness and warm rolling to 2 mm thickness and heat treatment may be attributed to formation of very fine and more homogeneously distributed $Fe_3AlC_{0·05}$ precipitate (figures 4b and c) as compared to hot-rolled 12 mm thick ESR alloy (figure 4a) due to the breaking of the precipitate by greater amount of working or may be due to the formation of fine grains by recrystallization (figure 4).

The high tensile elongation of all the four (alloys 1–4) ESR hot-rolled alloys at 873 K as compared to room temperature may be attributed to the increased dislocation mobility at higher temperature and is related to the change in failure mode from cleavage to the more ductile dimple.

4. Conclusions

(I) As-rolled ESR Fe–10·5Al–0·8C alloy exhibits a two-phase microstructure consisting of (a) Fe–Al with disordered *bcc* structure and (b) $Fe_3AlC_{0·5}$ precipitates. Addition of cerium to Fe–10·5Al–0·8C alloy resulted in the same phases, in addition to small volume fraction of cerium–oxycarbide precipitate.

(II) Small amount (0·01–0·04 wt.%) of cerium addition to Fe–10·5Al–0·8C alloy resulted in a significant improvement (1·8–4·1%) in room temperature tensile elongation. Further improvement in tensile elongation from 4·1–6·4% was achieved by increasing the cerium content from 0·04–0·2 wt.%.

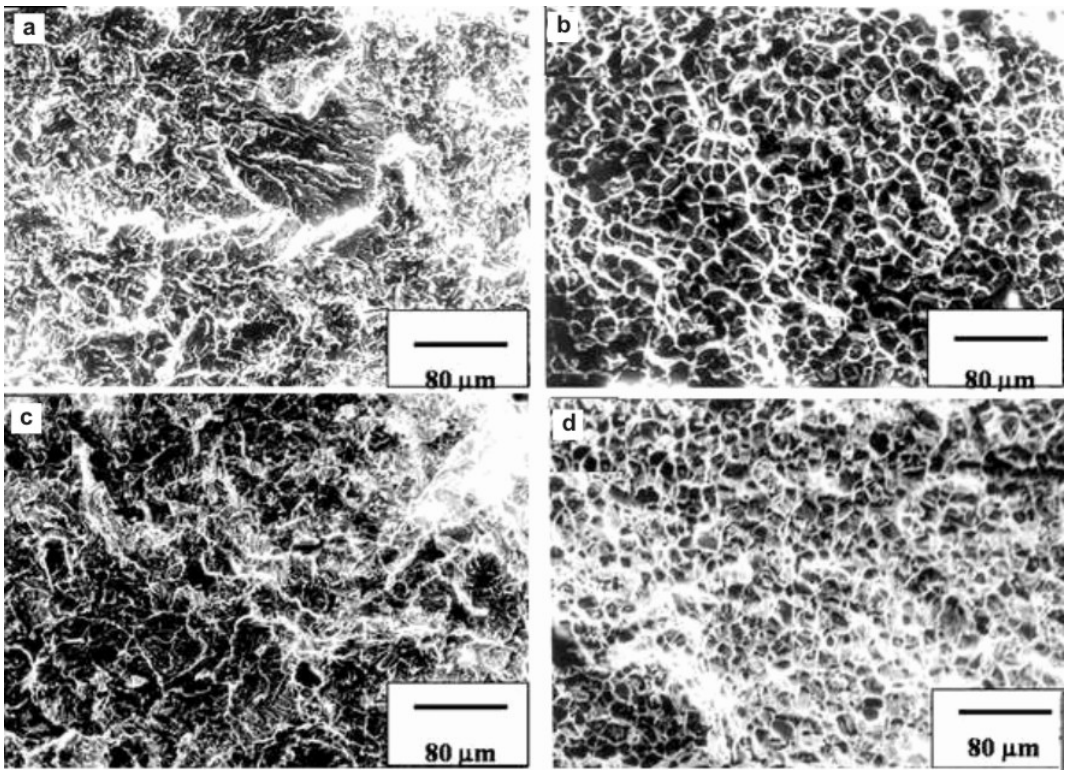

Figure 6. SEM fractographs showing the change in tensile fracture mode from transgranular cleavage (**a** & **c**) at room temperature to ductile dimple (**b** & **d**) at 873 K in hot-rolled ESR. (**a** & **b**) Fe–10·5Al–0·8C and (**c** & **d**) Fe–10·5Al–0·8C–0·2Ce alloys.

(III) Addition of cerium (0·01–0·2 wt.%) to Fe–10·5Al–0·8C alloy did not result in any significant improvement of the room and high-temperature strength as well as creep properties.

(IV) Warm-rolling and heat treatment of ESR hot-rolled alloy Fe–10·5Al–0·8C has resulted in further increase in tensile elongation from 6·4–10%.

Acknowledgements

The authors are grateful to the Defence Research and Development Organization, Ministry of Defence, New Delhi, for financial support in carrying out this research work. The authors wish to thank Dr D Banerjee, DRDO, New Delhi, Dr G Malakondaiah, Director, DMRL, for their interest and encouragement. The authors would like to thank fellow officers and staff of various groups of DMRL such as ERG (melting and casting), MEG (sample making), MWG (forging and rolling), MBG (tensile and creep testing) and SFAG (Metallography) for support.

References

Baligidad R G and Radhakrishna A 2002a *J. Mater. Sci.* **37** 5021

Baligidad R G and Radhakrishna A 2002b *J. Mater. Sci. Lett.* **21** 1231

Baligidad R G, Prakash U, Radhakrishna A, Rao P K and Ballal N B 1994 *Ironmaking Steelmaking* **21** 324

Baligidad R G, Prakash U, Radhakrishna A, Ramakrishna Rao V, Rao P K and Ballal N B 1996 *ISIJ Int.* **36** 1215

Baligidad R G, Prakash U and Radhakrishna A 1997 *Mater. Sci. Eng.* **A231** 206

Baligidad R G, Prakash U and Radhakrishna A 1998a *Mater. Sci. Eng.* **A255** 162

Baligidad R G, Prakash U and Radhakrishna A 1998b *Intermetallics* **6** 765

Chiu L H, Lee P Y and Chang C L 2000 *Mater. Manuf. Process* **15** 807

Khaple Shivkumar, Baligidad R G and Rao S 2007 *Mater. Sci. & Technol.* **23** 930

Khaple Shivkumar *et al* 2006 Technical Report 410, DMRL, Hyderabad, India

Kratochvil P, Karlik M, Hausild P and Cieslar M 1999 *Intermetallics* **7** 847

Mendiratta M G, Ehlers S K, Dimiduk D M, Kerr W R, Mazdiyasni S and Lipsitt H A 1987 in *High-temperature ordered intermetallic alloys II* (eds) N S Stoloff *et al* (MRS: Pittsburgh, Pennsylvania), **Vol. 81**, pp 393–405

McKamey C G and Liu C T 1990 *Scr. Metall.* **24** 2119

Schneider A, Falat L, Sauthoff G and Frommeyer G 2005 *Intermetallics* **13** 1322

Schwaiger A *et al* 2003 *Metal Powder Report* **58** 32

Stoloff N S 1998 *Mater. Sci. Eng.* **A258** 1

Yangshan S, Zhengjun Y, Zhonghua Z and Haibo H 1995 *Scr. Metall. Mater.* **33** 811

Yangshan S, Zhonghua Z, Feng X and KunZhong W 1996 *J. Mater. Sci. Lett.* **15** 820